

Nucleosynthesis in High-Entropy Hot-Bubbles of SNe and Abundance Patterns of Extremely Metal-Poor Stars

Natsuko Izutani¹ and Hideyuki Umeda¹

¹*Department of Astronomy, School of Science, University of Tokyo, Hongo, Tokyo 113-0033, Japan*

izutani@astron.s.u-tokyo.ac.jp; umeda@astron.s.u-tokyo.ac.jp

Accepted to ApJL: July 21, 2010

ABSTRACT

There have been suggestions that the abundance of Extremely Metal-Poor (EMP) stars can be reproduced by Hypernovae (HNe), not by normal supernovae (SNe). However, recently it was also suggested that if the innermost neutron-rich or proton-rich matter is ejected, the abundance patterns of ejected matter are changed, and normal SNe may also reproduce the observations of EMP stars. In this letter, we calculate explosive nucleosynthesis with various Y_e and entropy, and investigate whether normal SNe with this innermost matter, which we call “hot-bubble” component, can reproduce the abundance of EMP stars. We find that neutron-rich ($Y_e = 0.45-0.49$) and proton-rich ($Y_e = 0.51-0.55$) matter can increase Zn/Fe and Co/Fe ratios as observed, but tend to overproduce other Fe-peak elements.

In addition to it, we find that if slightly proton-rich matter with $0.50 \leq Y_e < 0.501$ with $s/k_b \sim 15-40$ is ejected as much as $\sim 0.06 M_\odot$, even normal SNe can reproduce the abundance of EMP stars, though it requires fine-tuning of Y_e . On the other hand, HNe can more easily reproduce the observations of EMP stars without fine-tuning. Our results imply that HNe are the most possible origin of the abundance pattern of EMP stars.

Subject headings: nuclear reactions, nucleosynthesis, abundances - supernovae: general

1. Introduction

The observational trends of extremely metal-poor (EMP) stars reflect SN nucleosynthesis of Population (Pop) III, or almost metal-free stars. Their observed abundances show

quite interesting patterns. There are significant differences between the abundance patterns in the iron-peak elements below and above $[\text{Fe}/\text{H}] \sim -2.5$. For $[\text{Fe}/\text{H}] \lesssim -2.5$, the mean value of $[\text{Cr}/\text{Fe}]$ and $[\text{Mn}/\text{Fe}]$ decrease toward lower metallicity, while $[\text{Co}/\text{Fe}]$ and $[\text{Zn}/\text{Fe}]$ increase (McWilliam et al. 1995; Cayrel et al. 2004).

Umeda & Nomoto (2002, 2005) and Tominaga, Umeda & Nomoto (2007) show that these trends can be related to the variations of explosion energy of core-collapse SNe, i.e, high $[\text{Zn}, \text{Co}/\text{Fe}]$ and low $[\text{Cr}, \text{Mn}/\text{Fe}]$ can be explained by a high energy SN (‘hypernova’), while low $[\text{Zn}, \text{Co}/\text{Fe}]$ and high $[\text{Cr}, \text{Mn}/\text{Fe}]$ by a normal SN. On the other hand, Heger & Woosley (2008) studied the evolution and parameterized explosions of Pop III stars with masses ranging from 10 to 100 M_{\odot} . They have concluded that the EMP stars do not show the need for a HN component, and that explosion energies less than 1.2 B seem to be preferred, though their models tend to underproduce Co and Zn.

These previous works do not include any contribution from hot bubbles in the innermost region of SNe. However, recent multi-dimensional simulations have shown that both the neutron-rich and proton-rich matter in hot-bubbles are ejected from the hot-bubble regions (e.g., Janka et al. 2003). This innermost matter with various Y_e and entropy is considered to be the origin of the heavier elements than Zn, but also can be the important site for the lighter elements (e.g., Hoffman et al. 1996). Heger & Woosley (2008) suggest that Co and Zn in their models can be enhanced by this innermost matter.

Our previous work, Izutani, Umeda & Tominaga (2009) have studied nucleosynthesis of lighter neutron-capture elements (weak r-process elements), Sr, Y, and Zr by considering small amount of mass ejection from below the conventional mass-cut, or from the hot-bubble regions. In that paper, we assumed that the “hot-bubble” matter has the same entropy with the supernova shock, though in reality it may have higher entropy (e.g., in Janka et al. 2003 the hot-bubble matter has the entropy in the range, $s/k_b \sim 30-50$). We have found that HN models with neutron-rich matter can reproduce these elements, but normal SN models cannot when we assume the same entropy with the supernova shock for the matter below the mass-cut. However, from the observational trends of $[\text{Zn}/\text{Fe}]$ and $[\text{Sr}/\text{Fe}]$ (see Figure 15 and Discussion in Izutani et al. 2009), it is highly possible that the main origin of the weak r-process is normal SNe. In addition to it, some weak r-process stars have also Mo, Ru, and Rh, though HN model cannot reproduce those elements. Therefore, we need to consider higher-entropy calculations to clarify the origin of these elements.

In this letter, we perform similar calculations as Izutani et al. (2009) with wider range of Y_e and entropy. We discuss whether normal SNe with the high-entropy hot-bubble component can reproduce the observations of EMP stars especially paying attention to Fe-peak elements. We also discuss some implications for the origin of the weak r-process elements, Sr-Rh.

2. MODEL & METHOD

The calculation method and other assumptions are the same as described in Umeda & Nomoto (2002, 2005) and Izutani et al. (2009) except for the size of the nuclear reaction networks. In this paper, we adopt the Pop III progenitors as in Umeda & Nomoto (2002, 2005) and apply the model with $M = 15 M_{\odot}$ and $E_{51} = 1$ (normal SN model) and $M = 25 M_{\odot}$ and $E_{51} = 20$ (HN model). Detailed nucleosynthesis is calculated as a postprocessing after the hydrodynamical calculation with a simple α -network. The isotopes included in the post-process calculations for $Y_e < 0.51$ are 809 species up to ^{121}Pd , and the ones for $Y_e \geq 0.51$ are 652 species up to ^{112}Pd . (for detail, see Izutani, Umeda & Yoshida (2010) in preparation). As for the HN model, we consider a model for which the density in the complete Si-burning region is artificially reduced to 1/3 (or entropy is enhanced by a factor of 3) of the original as well as the original model. The HN model with the entropy enhanced by a factor of 3 fits the observation from Ca to Zn except Cr as shown in Figure 1. We call this model “HN3 model” ($s/k_b \sim 50$), and call the HN model with the original entropy “HN model” ($s/k_b \sim 15$). As for the normal SN model, the density for the postprocessing is multiplied by factors of 1 ($s/k_b \sim 5$), 1/3 ($s/k_b \sim 15$), 1/10 ($s/k_b \sim 40$), and 1/35 ($s/k_b \sim 150$). This modification of density mimics hot-bubbles in multi-dimensional simulations.

We obtain the final yields by adding matter above M_{cut} and below M_{cut} . We set $M_{\text{cut}} = 1.50 M_{\odot}$ for the normal SN model and $1.88 M_{\odot}$ for the HN3 model. As a result, the normal SN model ejects $0.07 M_{\odot}$ of ^{56}Ni , which is similar to SN1987A, and the HN3 model ejects $0.51 M_{\odot}$ of ^{56}Ni .¹

3. Abundance Patterns of Whole Ejecta with Mass Ejection below M_{cut}

In Figure 1, the abundance patterns from Si to Ru are compared with those of EMP stars. As for Co and Zn, the HN3 model reproduces the observations well, while the normal SN model does not as described in the figure caption. As for Sr, Y, and Zr, both the HN3 model with neutron-rich hot-bubble matter ($s/k_b \sim 15$) and the normal SN model with neutron-rich hot-bubble matter reproduce the observations well. However, as for the heavier elements, Mo, Ru, and Rh, only the normal SN model with $s/k_b \sim 150$ neutron-rich hot-bubble matter reach the observations.

¹In the models assuming mixing-fallback effects, the actual amount of the ejected ^{56}Ni mass is smaller than this value. See Umeda & Nomoto (2005).

4. Parameter Dependence of Nucleosynthesis

In this section, we show parameter dependences of the products in hot-bubbles. In Figure 2, we show $[\text{Co,Zn/Fe}]$ vs Y_e . We show only the cases with $0.50 \leq Y_e \leq 0.501$ in Figure 2 because matter with Y_e in this range shows better fitting to the abundance of EMP stars than neutron-rich ($0.45 \leq Y_e \leq 0.49$) and proton-rich ($0.51 \leq Y_e \leq 0.55$) matter as mentioned in the next paragraph. $[\text{Co/Fe}]$ once increases as Y_e increases, but decreases for larger Y_e in all the SN models. Y_e at the $[\text{Co/Fe}]$ peak becomes larger with higher entropy. $[\text{Co/Fe}]$ has the peak at $Y_e = 0.5003, 0.5004,$ and 0.5005 for $s/k_b \sim 5, 15,$ and $40,$ respectively. $[\text{Co/Fe}]$ becomes higher with higher entropy. The highest $[\text{Co/Fe}]$ is $\sim 0.5, 0.7,$ and 0.9 for $s/k_b \sim 5, 15,$ and $40,$ respectively. $[\text{Zn/Fe}]$ is nearly 0 in regardless of Y_e when $s/k_b \sim 5,$ but decreases as Y_e increases in the higher-entropy ($s/k_b \sim 15$ and 40) cases. $[\text{Zn/Fe}]$ becomes higher with higher entropy. For example, $[\text{Zn/Fe}]$ is $\sim 0.1, 0.4,$ and 0.9 with $Y_e = 0.50$ for $s/k_b \sim 5, 15,$ and $40,$ respectively. For comparison, we also show $[\text{Zn,Co/Fe}]$ in the complete Si-burning region of the HN3 model by the horizontal lines.

Neutron-rich matter ($0.45 \leq Y_e \leq 0.49$) also produces Co and Zn to some extent, but at the same time, tends to overproduce Ni (Figure 3). EMP stars show $[\text{Co/Ni}] \gtrsim 0,$ while neutron-rich matter shows $[\text{Co/Ni}] < 0.$ Proton-rich low-entropy matter also produces Co and Zn, but the abundance of Co is smaller than the case with $0.50 \leq Y_e \leq 0.501.$ Proton-rich high-entropy matter produces less Co and Zn than proton-rich low-entropy matter. In addition to it, both neutron- and proton-rich matter tend to overproduce Cu.

5. Trends of Fe-peak Elements of Whole Ejecta

Here, we describe in detail the abundance patterns of Fe-peak elements in the whole ejecta with mass ejection below M_{cut} or with hot-bubble component. For the matter below $M_{\text{cut}},$ the yields are averaged for Y_e values ranging from 0.45 to 0.50 for neutron-rich matter, and from 0.51 to 0.55 for proton-rich matter. The entropy below M_{cut} is fixed. The other parameter of our model is the mass of ejected matter from the regions below $M_{\text{cut}}, \Delta M.$ ΔM is added to the matter above $M_{\text{cut}},$ and they are assumed to be ejected to the outer space all together.

Figure 3 shows comparison between observed $[\text{Co/Fe}], [\text{Ni/Fe}]$ vs. $[\text{Zn/Fe}]$ and those in our models. These ratios are the ones of the total ejecta. Therefore, the trends of their values are similar with the ones seen in Figure 2, but on the other hand, their exact values are different between Figure 2 and Figure 3 because the total ejecta includes the incomplete Si-burning region where Fe is produced, but Co and Zn are not. For example, $[\text{Zn/Fe}]$ is \sim

0.6, and $[\text{Co}/\text{Fe}]$ is ~ 0.2 in the total ejecta of HN3 (open cyan triangle in Figure 3), while $[\text{Zn}/\text{Fe}]$ is ~ 0.9 , and $[\text{Co}/\text{Fe}]$ is ~ 0.4 in the complete Si-burning region (blue and magenta horizontal lines in Figure 2).

The gradient of $[\text{Co}/\text{Fe}]$ vs. $[\text{Zn}/\text{Fe}]$ in EMP stars is larger than that of the normal SN models with hot-bubble component. The normal SN models with neutron-rich ($0.45 \leq Y_e \leq 0.50$) matter (indicated by blue circles) show the best Co/Zn among all the normal SN models. However, Figure 3 right panel shows that the normal SN models with neutron-rich matter tend to overproduce Ni (see also the caption of Figure 3) as also mentioned in Section 4, though $[\text{Ni}/\text{Fe}]$ in EMP stars with $[\text{Zn}/\text{Fe}] = 0.2\text{-}0.3$ is well reproduced if neutron-rich matter is added a little ($\lesssim 0.006 M_\odot$). On the other hand, the HN3 model is marginally consistent with the observed $[\text{Co}/\text{Fe}]$, and reproduces the observed $[\text{Ni}/\text{Fe}]$ well. In Figure 3, we also plot the ratios for the SN models with $Y_e = 0.50$, 0.5004, and 0.501 with $s/k_b \sim 15$ (red filled circles), and $Y_e = 0.50$, 0.5005, and 0.502 with $s/k_b \sim 40$ (magenta filled circles). We show $Y_e = 0.5004$ for $s/k_b \sim 15$ matter, and $Y_e = 0.5005$ for $s/k_b \sim 40$ matter because $[\text{Co}/\text{Fe}]$ has its peak at this Y_e value in each case. When $s/k_b \sim 15$, $[\text{Co}/\text{Fe}]$ has its peak value (~ 0.4) at $Y_e = 0.5004$, and $[\text{Co}/\text{Fe}]$ decreases with higher Y_e . $[\text{Co}/\text{Fe}]$ is ~ -0.1 at $Y_e = 0.501$. The similar trend of $[\text{Co}/\text{Fe}]$ and Y_e can be seen when $s/k_b \sim 40$. These trends are consistent with the ones shown in Figure 2.

As for the HN model and the HN3 model, we also show a version, where the complete Si-burning region is set to be $Y_e = 0.5001$ (see Umeda & Nomoto 2005). In this version, $[\text{Co}/\text{Fe}]$ becomes higher, and the HN models reproduce the observations well. For example, $[\text{Zn}/\text{Fe}]$ is ~ 0.6 , and $[\text{Co}/\text{Fe}]$ is ~ 0.2 in the HN3 model with $Y_e = 0.50$ (cyan open triangle with letters “HN3 0.50” in Figure 3), while $[\text{Zn}/\text{Fe}]$ is ~ 0.6 , and $[\text{Co}/\text{Fe}]$ is ~ 0.3 in the HN3 model with $Y_e = 0.5001$ (cyan open triangle with letters “HN3 0.5001” in Figure 3).

6. Discussion

In this letter we have confirmed that only hypernova type mass ejection can reproduce abundance of Fe-peak elements in EMP stars, and neither neutron- or proton-rich high-entropy matter ejection can help. This also means that if normal SNe eject hypernova-like matter below M_{cut} , then even normal SNe can reproduce $[\text{Co}, \text{Zn}/\text{Fe}]$ in EMP stars. More quantitatively, we find that the observations require ejection of as much as $0.06 M_\odot$ matter with $Y_e = 0.500\text{-}0.501$ with $s/k_b \sim 15\text{-}40$. This condition may be difficult to realize for a normal SN. For example, according to Janka et al. (2003), in their models the amount of $Y_e < 0.47$, ≤ 0.50 , and > 0.50 matter is $< 10^{-4} M_\odot$, $6 \times 10^{-3} M_\odot$, and $0.03 M_\odot$, respectively, and only small fraction of matter is in the range of $Y_e = 0.500\text{-}0.501$. Therefore, this solution

seems too contrived, though SN explosion mechanism is still uncertain and thus we cannot conclusively deny such a possibility.

Here we discuss the additional cases with the different timescales, the time it takes the flow to cool from some temperature to lower temperature. As a result, $[\text{Co}/\text{Fe}]$ is changed by the timescale below $T = 4 \times 10^9$ K (Pruet et al. 2005). The timescale below $T = 4 \times 10^9$ K multiplied by a factor of 1/2 and 2 gives $[\text{Co}/\text{Fe}] \sim 0.5$ and 0.2, respectively, while $[\text{Co}/\text{Fe}] \sim 0.4$ in the case with the original timescale as mentioned in Section 5. However, Ye range and ejected mass needed is not so changed; the upper limit of Ye becomes a little larger, $Ye \sim 0.502$, and ejected mass, a little smaller $\sim 0.03 M_{\odot}$.

There is another reason why SN models are not favored to explain large $[\text{Co,Zn}/\text{Fe}]$ stars. As mentioned in Introduction, $[\text{Co}/\text{Fe}]$ decreases with higher metallicity, and many stars show $[\text{Co}/\text{Fe}] \sim 0$ when $[\text{Fe}/\text{H}] \gtrsim -2.5$. At this age, only core-collapse SNe are considered to contribute to interstellar matter from the observation of $[\alpha\text{-elements}/\text{Fe}]$. If the typical value of $[\text{Co}/\text{Fe}]$ in normal SN is ~ 0.3 , $[\text{Co}/\text{Fe}]$ does not decrease to ~ 0 at $[\text{Fe}/\text{H}] \sim -2.5$. On the other hand, IMF average of the supernova ejecta can be $[\text{Co,Zn}/\text{Fe}] \sim 0$ even though HN models have large $[\text{Co,Zn}/\text{Fe}]$ (Tominaga et al. 2007).

Therefore, we suggest that Co and Zn in EMP stars originated from HNe, not from normal SNe. As for weak r-process elements, it is not clear that Sr-Zr rich weak r-process stars are always Mo-Rh rich. Observational data of both Sr-Zr and Mo-Rh are obtained in only two weak r-process stars HD122563 and HD88609 (Honda et al. 2007). Sr-Zr are produced in neutron-rich hot-bubble of $s/k_b \sim 15$, while both Sr-Zr and Mo-Rh are produced in neutron-rich hot-bubble of $s/k_b \sim 150$, that may be the part of neutrino-driven wind, rather than hot-bubble component (Roberts et al. 2010). Of course, this work is only parametric search, and some other possibilities may exist in reality. Further investigation is needed to disclose the origin of the abundances in EMP stars.

This work was partly supported by Grants-in-Aid for JSPS Fellows.

REFERENCES

- Cayrel, R. et al. 2004, A&A, 416, 1117
 Francois, P. et al. 2007, A&A, 476, 935
 Heger, A., & Woosley, S. E. 2008, submitted to ApJ (preprint at arXiv:0803.3161)
 Hoffman, R. D., Woosley, S. E., Fuller, G. M., Meyer, B. S. 1996, ApJ, 460, 478

- Honda, S., Aoki, W., Ishimaru, Y., Wanajo, S. 2007, ApJ, 666, 1189
- Izutani, N., Umeda, H., & Tominaga, N. 2009, ApJ, 692, 1517
- McWilliam, A. et al. 1995, AJ, 109, 2757
- Pruet, J., Woosley, S. E., Buras, R., Janka, H.-T., & Hoffman, R. D., 2005, ApJ, 623, 325
- Roberts, L. F., Woosley, S. E., & Hoffman, R. D. 2010, submitted to ApJ (preprint at arXiv:1004.4916)
- Tominaga, N., Umeda, H., & Nomoto, K. 2007, ApJ, 660, 516
- Umeda, H., & Nomoto, K. 2002, ApJ, 565, 385
- Umeda, H., & Nomoto, K. 2005, ApJ, 619, 427

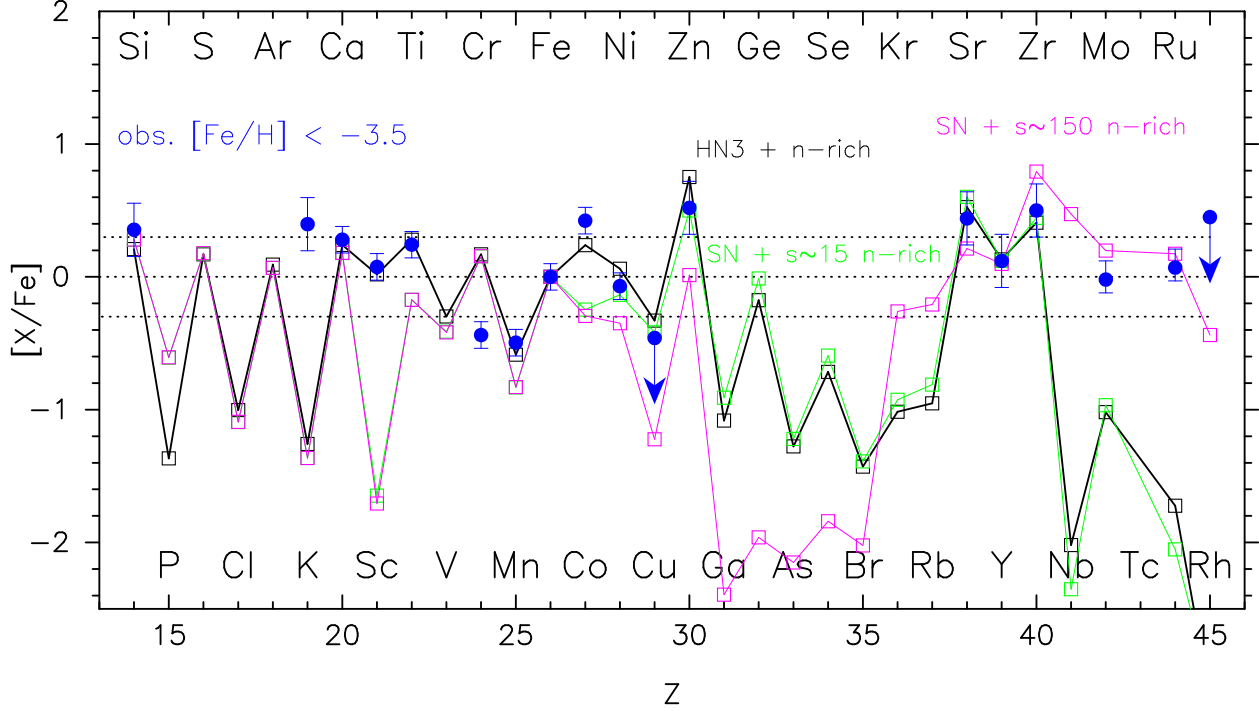


Fig. 1.— Comparison between the yields of our models (HN3 model: black lines; SN model with $s/k_b \sim 15$ neutron-rich matter: green lines; SN model with $s/k_b \sim 150$ neutron-rich matter: magenta lines) and the abundance patterns of the EMP stars (blue circles with error bars). The observations from Si to Zn are the average of four EMP stars with $-4.2 < [Fe/H] < -3.5$ from Cayrel et al. (2004). The observations from Sr to Zr, and from Mo to Rh are the ones of CS 22897-008 (François et al. 2007) and HD 122563 (Honda et al. 2007), respectively. Among them, only the HN3 model reproduces both Co and Zn. In addition to it, the HN3 model may reproduce Sr, Y, and Zr if hot-bubble component is added as Izutani et al. (2009). The normal SN model with $s/k_b \sim 15$ neutron-rich matter has high ratio of Zn, but Co is not good. The normal SN model with $s/k_b \sim 150$ neutron-rich matter reproduces not only $[Sr, Y, Zr/Fe] \sim 0$, but also $[Mo, Ru, Rh/Fe] \sim 0$. The models with proton-rich matter reproduce neither Co nor weak r-process elements, which we do not show in this figure.

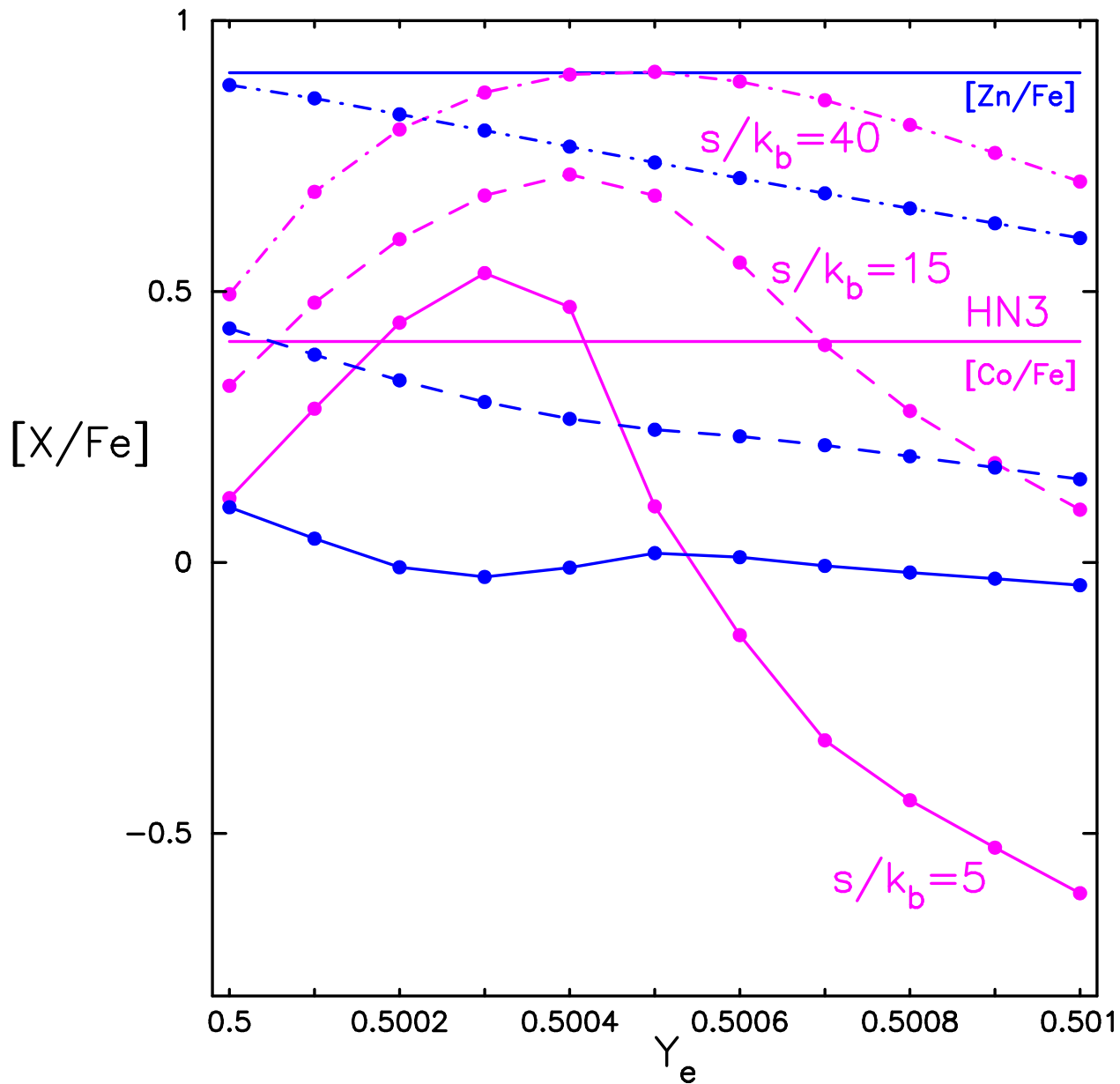


Fig. 2.— $[Co,Zn/Fe]$ in “hot-bubbles” of SNe. $[Co/Fe]$ and $[Zn/Fe]$ are represented by magenta and blue figures, respectively. The ratios for $s/k_b \sim 5$ (original), 15, and 40 flows in the normal SN model are represented by solid, dashed, and dash-dotted lines, respectively. The horizontal lines indicate the ratios in the HN3 model with the original Y_e , 0.50.

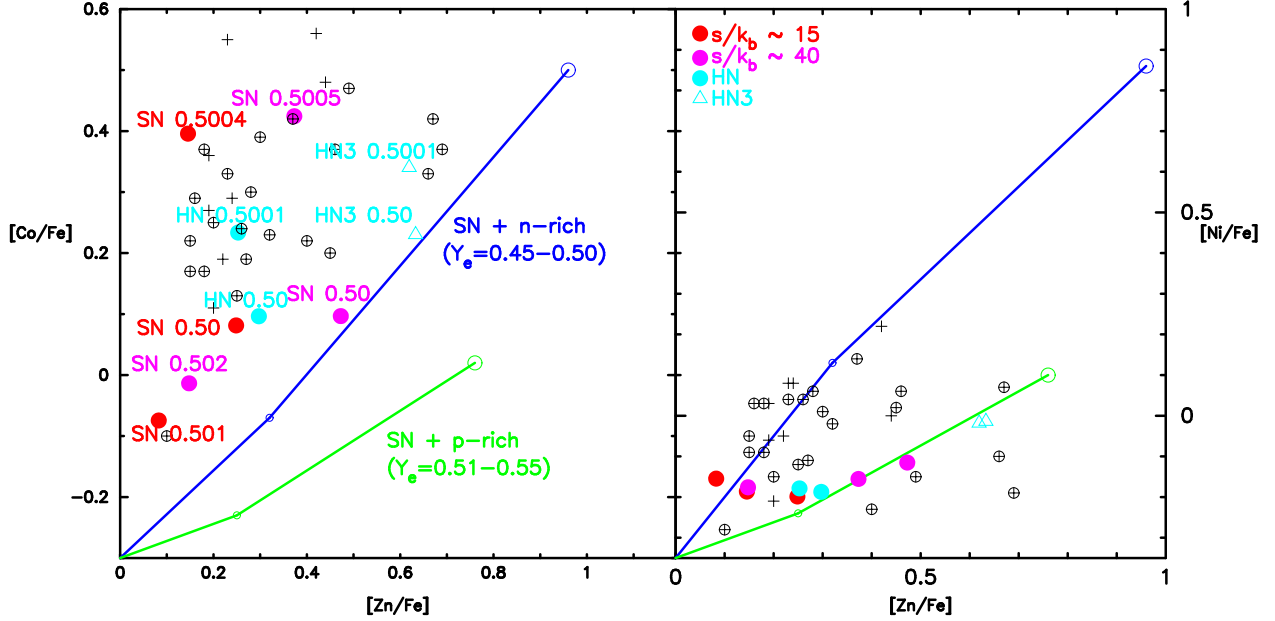


Fig. 3.— Comparison between observed abundance ratios and those in our models. Left panel: $[\text{Co}/\text{Zn}]$ vs. $[\text{Zn}/\text{Fe}]$. Right panel: $[\text{Ni}/\text{Fe}]$ vs. $[\text{Zn}/\text{Fe}]$. The observations are represented by black crosses. The observations with high $[\text{Sr}/\text{Ba}]$ and $[\text{Y}/\text{Eu}]$ (weak-r process star: see Izutani et al. 2009 for detail) are enclosed by black circles. The ratios for the normal SN model with neutron-rich and proton-rich matter are represented by blue and green circles, respectively. Small and big circles indicate the models with $\Delta M = 0.006 M_{\odot}$ and $0.06 M_{\odot}$, respectively. For the SN models, we show only the original entropy models because they have better $[\text{Co}/\text{Fe}]$ than higher entropy models. All the SN models with a hot-bubble component do not reach the observations of $[\text{Co}/\text{Fe}]$. Among them, the SN model with neutron-rich matter ($Y_e = 0.45-0.50$) of $s/k_b = 5$ shows the best Co/Zn ($[\text{Co}/\text{Fe}] \sim 0.3$ at $[\text{Zn}/\text{Fe}] \sim 0.7$) but tends to overproduce Ni ($[\text{Ni}/\text{Fe}] \sim 0.5$ at $[\text{Zn}/\text{Fe}] \sim 0.7$). The ratios for the HN models and the HN3 models are represented by cyan filled circles and open triangles, respectively. We also show the ratios for the SN models with $Y_e = 0.50, 0.5005$, and 0.502 with $s/k_b = 40$ (magenta filled circles), and the ratios for the SN models with $Y_e = 0.50, 0.5004$, and 0.501 with $s/k_b = 15$ (red filled circles). ΔM is $0.06 M_{\odot}$ in these 6 models. The ratio for the normal SN model without hot-bubbles is located at the coordinate origin.